

## Photochemical Degradation of Poly(ethylene Terephthalate). IV. Surface Changes

P. BLAIS, M. DAY, and D. M. WILES, *Division of Chemistry, National Research Council of Canada, Ottawa, Canada*

### Synopsis

The chemical, physical, and mechanical changes in the surface properties of poly(ethylene terephthalate) film produced by ultraviolet light have been examined. Attenuated total reflection infrared spectroscopy has indicated that numerous chemical scission reactions occur in the front surface layer facing the source of irradiation, resulting in the formation of carboxylic acid endgroups. This preferential surface photodegradation has been confirmed by examining the cross section of irradiated film by electron beam-induced luminescence. Conventional electron microscopy revealed little changes in the surface appearance of irradiated film. However, indirect techniques were devised which indicated that changes do occur in the physical properties of the surface. These observed changes are believed to be responsible for the decrease in film tensile strength, which has been shown to be a surface phenomenon and not a bulk property.

### INTRODUCTION

The photodegradation of poly(ethylene terephthalate) (PET) film is a complex process involving both photolysis and photo-oxidative reactions.<sup>1</sup> These reactions involve chain scissions, resulting predominantly in the formation of the gaseous products CO and CO<sub>2</sub> and carboxylic acid (—COOH) endgroups. Associated with these chemical reactions occurring within polymer molecules, physical changes also take place which result in a deterioration of the mechanical properties. These processes have been monitored under a variety of artificial light exposure conditions, and the results have been reported.<sup>2,3</sup> These investigations revealed that the changes in the physicomechanical properties were occurring at a faster rate than the changes in the bulk chemical properties. These changes were found to parallel the surface chemical changes. It was felt, therefore, that a more detailed investigation of the surface of photodegraded PET should be undertaken in an attempt to relate the chemistry of the polymer surface to other parameters that may have an effect on the bulk mechanical properties.

In this work, changes in the surface chemical composition of PET films were studied by attenuated total reflection (ATR) infrared (IR) spectroscopy. Changes in the surface morphology were investigated using electron microscopy. Both techniques were used to ascertain the extent to

which the surface had been damaged in an attempt to rationalize the loss of mechanical strength.

ATR IR spectroscopy is an established technique for studying surface chemistry of polymers and has been used previously in this laboratory.<sup>4-6</sup> Essentially, the technique enables the spectra of a sample surface to be recorded by placing it in direct contact with an optically denser but transparent reflecting element.<sup>7</sup> The depth of penetration of the IR beam into the sample is dependent upon the choice of reflecting element and angle of incidence of the beam into the sample. Variations in these parameters enable the IR beam to penetrate the surface to different predetermined depths<sup>8</sup> in the range of 0.1 to 2  $\mu$  approximately. It is thus possible to follow the extent of chemical changes in a polymer system as a function of distance into the sample from the surface and so construct partial concentration profiles.

Similar concentration profiles have also been obtained of the fluorescent material formed on photo-oxidation.<sup>2,3</sup> These have been achieved by using the scanning electron microscope (SEM) in which the conventional detection system which responds to the secondary electron emission from the surface has been replaced with a detection system which responds to the luminescent emission induced by the electron beam. Cross-sectional examination of such a film enables the distribution of this fluorescent product to be determined as a function of distance from the surface.

Physical changes in the surface layers which resulted from the photochemical degradation were investigated by electron microscopy. The approach used previously in this laboratory with isotactic polypropylene<sup>6</sup> was adapted to PET in an attempt to correlate chemical, structural, morphological, or textural changes in the surface with mechanical properties of the bulk polymer.

## EXPERIMENTAL

The PET film used in this work was 21  $\mu$  thick Mylar, supplied by du Pont, and reported to contain no light stabilizers. The number-average molecular weight ( $\bar{M}_n$ ) of the polymer was 19,700 and the density, 1.398. Several experiments involving the SEM were performed with 100  $\mu$  thick film of the same origin and type.

Irradiations were carried out using an Atlas xenon-arc Weather-Ometer (Model 600-WR).

The IR spectra were recorded using a Beckman IR8 double-beam spectrophotometer. Surface spectra were measured using a Wilks #9 ATR attachment (Wilks Scientific, Norwalk, Conn.) on the above instrument. The two reflection elements employed were germanium (Ge) and KRS-5 at nominal angles of incidence of 60°, 45°, and 30°. Quantitative data from these spectra were obtained from the optical density (O.D.) measurements of the carboxylic acid endgroup absorption centered at 3290  $\text{cm}^{-1}$  (assigned to the O—H vibration of the —COOH group<sup>2</sup>). The usual normalization

procedure was used in order to take into account variations in sample size, sample-to-element contact, and the number of internal reflections obtained by the use of different reflecting conditions.

Transmission electron microscopy (TEM) on these samples consisted in examining surface replicas (direct replicas) and replicas of interior surfaces exposed by the removal of a wetting adhesive layer (transfer replicas),<sup>6,9</sup> with the aid of a Philips 100 electron microscope. A Cambridge S-2 scanning electron microscope was used to assess gross surface damage and textural changes associated with the degradation. This instrument was also used to study some tensile fracture surfaces and transverse sections of PET films. Normal secondary emission mode images containing the usual topographic information were complemented by electron beam-induced luminescence distribution studies. To this end, the usual secondary electron detector was replaced by a nondispersive optical emission detector incorporating a photomultiplier (EMI 6255) having its maximum spectral response centered at a wavelength of 400 nm. This device would be regarded as a coarsely integrating optical detector since it could sum all visible photons emitted by the sample independently of their wavelength or decay lifetime.

## RESULTS AND DISCUSSION

### Infrared Data

Films of PET which are UV irradiated show changes in their IR absorption spectra<sup>2</sup> in the vicinity of  $3290\text{ cm}^{-1}$  owing to the formation of  $-\text{COOH}$  endgroups. Changes in the O.D. of this band within the polymer surface layers were followed as a function of UV exposure time by ATR spectroscopy. The surface was probed to different depths by choosing different reflecting elements (e.g., KRS-5 or Ge) and/or varying the angle of incidence of the IR beam with respect to the surface. Harrick<sup>7</sup> established the expression

$$d_p = \frac{\lambda}{2\pi n_1 [\sin^2\theta - (n_2/n_1)^2]^{1/2}} \quad (1)$$

linking the effective depth of penetration ( $d_p$ ) of an IR beam of wavelength  $\lambda$  into a film of refractive index  $n_1$  placed in contact with a reflecting element of refractive index  $n_2$ , where  $\theta$  is the angle of incidence of the IR beam at the film's surface. The  $d_p$  values imposed by the available reflection conditions in this investigation are given in Table I based on an absorption wavelength of  $3\ \mu$  ( $3290\text{ cm}^{-1}$ ) for the  $-\text{COOH}$  endgroup.

Samples of PET film were irradiated for various times, and the increase in the normalized O.D. values attributed to  $-\text{COOH}$  formation was monitored using the five different ATR conditions given in Table I. The results obtained for the surface facing the irradiation light source are shown in Figure 1. Also included in this figure are the data from the transmission

TABLE I  
ATR Conditions and Depths of Penetration

Reflection element	$n_{21}^a$	Angle of incidence		$d_p^d/\lambda_0$	$d_p$ at 3290 $\text{cm}^{-1}$ , $\mu$
		Nominal <sup>b</sup>	Actual <sup>c</sup>		
Ge	0.410	60	49	0.058	0.17
Ge	0.410	45	45	0.069	0.21
Ge	0.410	30	41	0.078	0.23
KRS-5	0.683	60	51	0.179	0.54
KRS-5	0.683	45	45	0.363	1.09

<sup>a</sup> Ratio of refractive indices of PET (1.64) to reflection element (Ge = 0.4, KRS-5 = 2.4).

<sup>b</sup> Not corrected for refraction at the entrance facet (45° bevel in all cases).

<sup>c</sup> True angle corrected for refraction.

<sup>d</sup> Depth of penetration calculated from eq. (1).

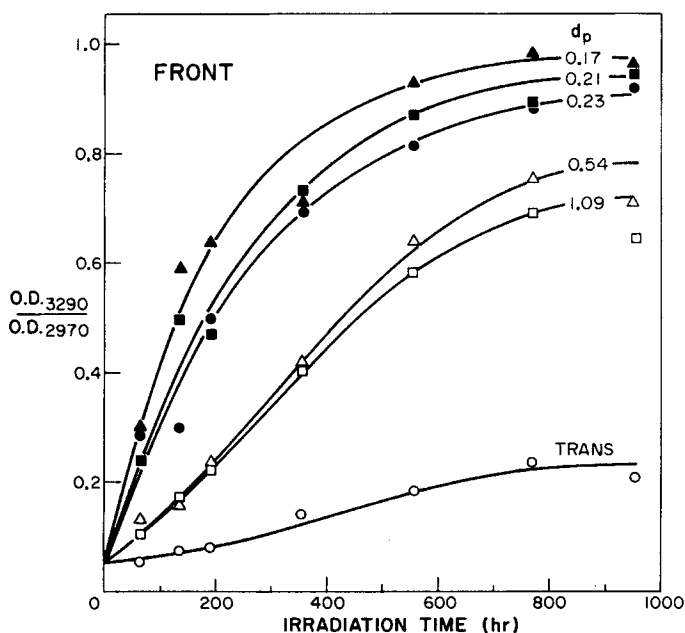


Fig. 1. Effect of irradiation time on normalized —COOH absorption at front surface.

IR measurements to give an indication of the total change throughout the film cross section. A similar series of curves was obtained for the surface facing away from the irradiation light source (Fig. 2). These two figures indicate that photodegradation is proceeding at a significant rate on the front surface, at a decreased rate on the rear surface, and at a negligible rate in the film interior. This distribution of photodegradation is conveniently illustrated by plotting variations in the normalized absorption of the —COOH endgroup as a function of depth of penetration. Figure 3 illustrates this rapid frontal degradation which increases with sustained

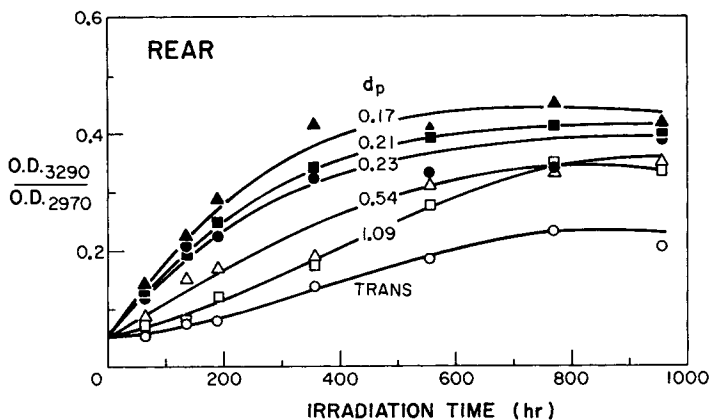


Fig. 2. Effect of irradiation time on normalized  $-COOH$  absorption at rear surface.

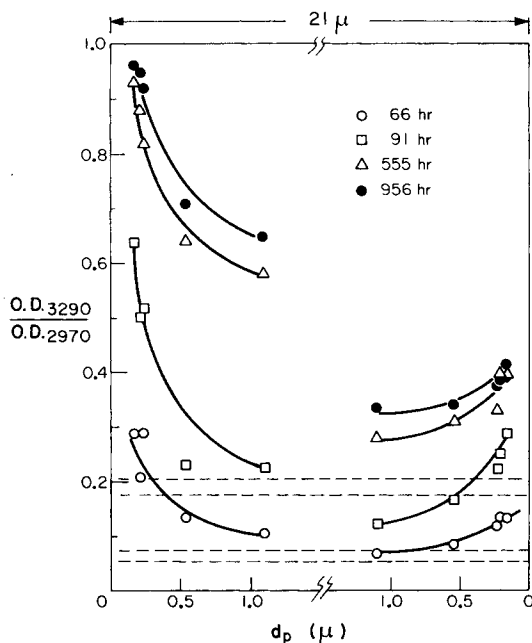


Fig. 3. Variation of normalized  $-COOH$  absorption with depth of penetration;  $d_p$  values measured in from each surface of the  $21\mu$  film. (---) Transmission values.

UV irradiation up to about 400 hr of exposure, after which only minor changes take place in the first  $0.5 \mu$  of depth. A similar but less pronounced effect can be seen for the rear surface. As irradiation proceeds, the thickness of the degraded surface layers gradually increases.

In order to appreciate the extent of this surface degradation, it is possible to calculate the extent of chain-breaking reactions required to produce these increases in the normalized O.D. values. In the unirradiated samples

TABLE II  
 Characteristics of PET Front Surface ( $d_p = 0.17 \mu$ ) as a  
 Function of Irradiation Time

Irradiation time, hr.	0	66	191	555	956
O.D. <sub>3290</sub> /O.D. <sub>2970</sub>	0.055	0.292	0.639	0.930	0.960
—COOH, $\times 10^6$ equiv g <sup>-1</sup>	41.4	219.9	481.2	700.3	722.9
New —COOH groups, $\times 10^6$ equiv g <sup>-1</sup>	0	178.5	439.8	658.9	681.5
Repeat units/polymer chain <sup>a</sup>	103	22	10	6	6
Repeat units/polymer chain <sup>b</sup>	103	11	5	3	3

<sup>a</sup> Based on Norrish type II formation of —COOH endgroups only.

<sup>b</sup> Assuming Norrish type I scissions occur at an equal rate to the Norrish type II process.

of PET film, a value of 0.055 for O.D.<sub>3290</sub>/O.D.<sub>2970</sub> has been shown<sup>3</sup> to correspond to an initial concentration of —COOH endgroups of 0.058 g equiv./l. (i.e.,  $41.4 \times 10^{-6}$  equivalents per gram of film). Based on a number-average molecular weight of 19,700, the average polymer chain consists of about 100 repeat units, with about 80% of the endgroups of the —COOH type. If it is assumed that the normalized O.D. values given in Figures 1, 2, and 3 are directly proportional to the concentration of —COOH endgroups, it is possible to estimate their approximate concentration in the various surface layers. These calculations have been made for the front surface layer of  $d_p = 0.17 \mu$ , and the results are listed in Table II. Since it has been shown<sup>1</sup> that the —COOH endgroups are formed mainly as a result of a Norrish type II photorearrangement reaction



each new acid endgroup represents one chain scission reaction. Estimates of the polymer chain lengths present in the front surface layer after degradation were thus calculated, and the results are shown in Table II. Although these calculations are oversimplified, the number of chain scissions is expected to be an underestimate since no consideration has been made for the alternative Norrish type I degradation route. This latter reaction would be expected to account for an equal number of chain scissions as those giving rise to —COOH endgroups, since both have approximately equal quantum yields.<sup>1</sup> Correcting for these Norrish type I reactions gives the results in the last row of Table II, where the possibility of photochemical decomposition of the —COOH endgroups in secondary reactions is neglected.

In a previous study,<sup>2</sup> it has been shown that an irradiation time of 600 hr is sufficient to embrittle the film. From Table II it can be concluded that the material in the first  $0.17 \mu$  consisted of oligomers of less than five repeat units. Such a material could have had few of the mechanical properties of the initial film. Consideration of this conclusion should include the various uncertainties inherent to the ATR IR technique. For example, the gross changes noted in the chemical nature of the film's surface would

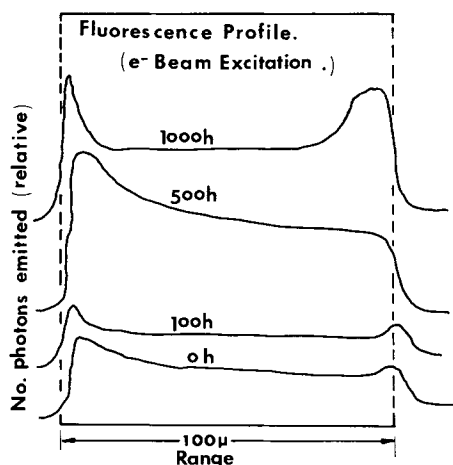
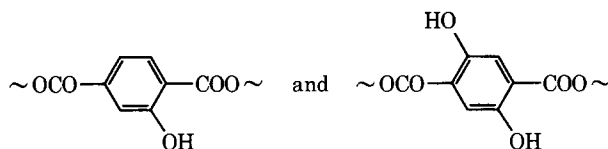


Fig. 4. Total luminescence intensity profile of 100 μ photo-oxidized PET films under electron beam excitation. Irradiated side on the left.

also be expected to alter its optical properties (i.e., the surface may have a gradually changing refractive index  $n_1$  as degradation proceeds). Consequently, several other techniques were used in an attempt to test the validity of the conclusion.

**Electron Beam-Induced Fluorescence**

Mono and dihydroxy terephthalate groups of the type:



showing fluorescence under UV excitation appear during the photo-oxidation of PET.<sup>10</sup> It was found that these compounds undergo similar fluorescence under electron beam excitation.<sup>11</sup> Consequently, the SEM was adapted to fulfill the role of fluorescence probe.

For the needs of this communication, it is sufficient to visualize this probe as a 0.1 μ beam of electrons, accelerated under 20 kV potential and directed at a point on the polymer sample. A photon counting device is used to measure visible light emission from that point. If such a point is scanned across a PET fracture or cross section, the emission intensity profile will reflect the concentration of the excited fluorescent species as a function of distance from the irradiated surface. Since the concentration of the hydroxy esters is related to the extent of photo-oxidation,<sup>2,10,11</sup> it thus follows that the magnitude of the fluorescent signal on scanning a cross section measures the UV damage at various depths in the film. A family of fluorescence profiles for films having received various exposures to UV is shown in Figure 4, which employs a shifting baseline for clarification. For

that purpose, the photo-oxidized  $100\ \mu$  thick films were cut edgewise with a fresh, grease-free razor blade, mounted vertically, coated with  $200\ \text{\AA}$  of evaporated carbon, and scanned across with the exciting beam. Although prone to larger errors than is ATR spectroscopy, this method yields the same general concentration profiles as before: a high concentration of products in the front surface layer (left side of Fig. 4) and a lesser amount in the interior. As observed previously with ATR, a gradual increase in photodegradation of the interior during prolonged exposure (viz., 500 hr) also occurs. Noteworthy in Figure 4 are the observations that even virgin film shows a fluorescence background and that extended UV exposure (i.e., 1000 hr) appears to reduce the fluorescence.

### Microscopy

The search for textural and physical damages associated with the photochemical deterioration of PET films by electron microscopy was surprisingly fruitless, even at high resolution. As seen in Figure 5, the initially featureless surface of PET remains featureless, even after prolonged UV exposure, with the exception that small amounts of particulate debris appeared on some areas of irradiated films.

A test for material losses (volatilization) or volume contraction was devised by leaving an opaque light shield with small apertures (a 300 mesh TEM grid) on the film surface during exposure. After prolonged exposure, it was found that the unshielded areas were depressed below the surface of the film, but that the shielded and unshielded areas had the same general

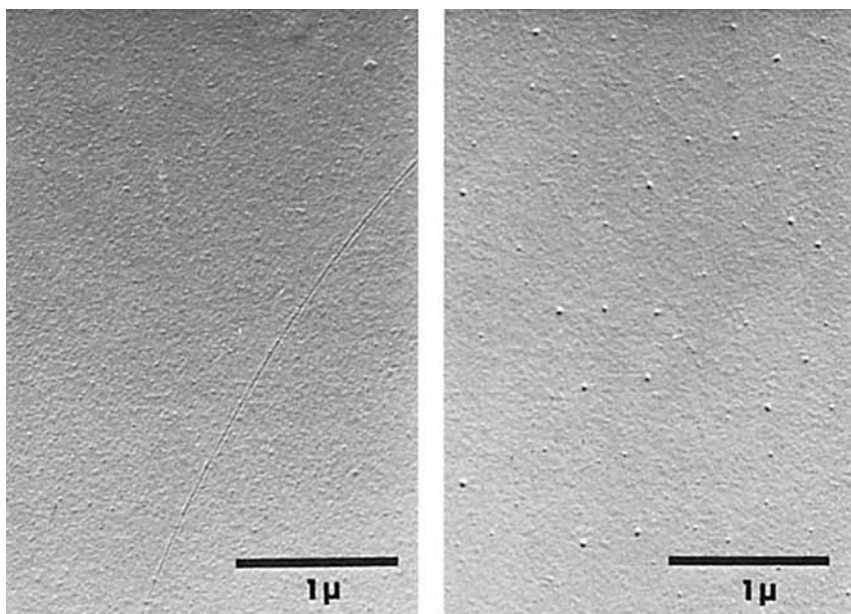


Fig. 5. Transmission electron micrographs of direct replica of PET surface: (a) unirradiated sample; (b) after 1000 hr of irradiation.



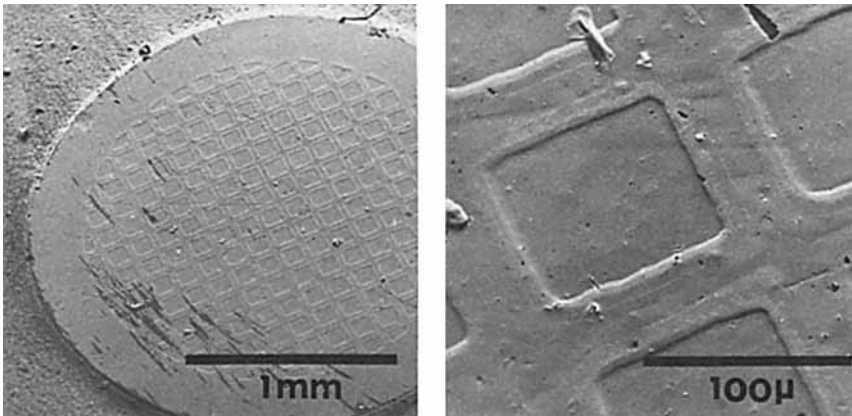


Fig. 6. Scanning electron micrographs of PET film surface shielded by a 300 mesh open grid during UV exposure (1000 hr).

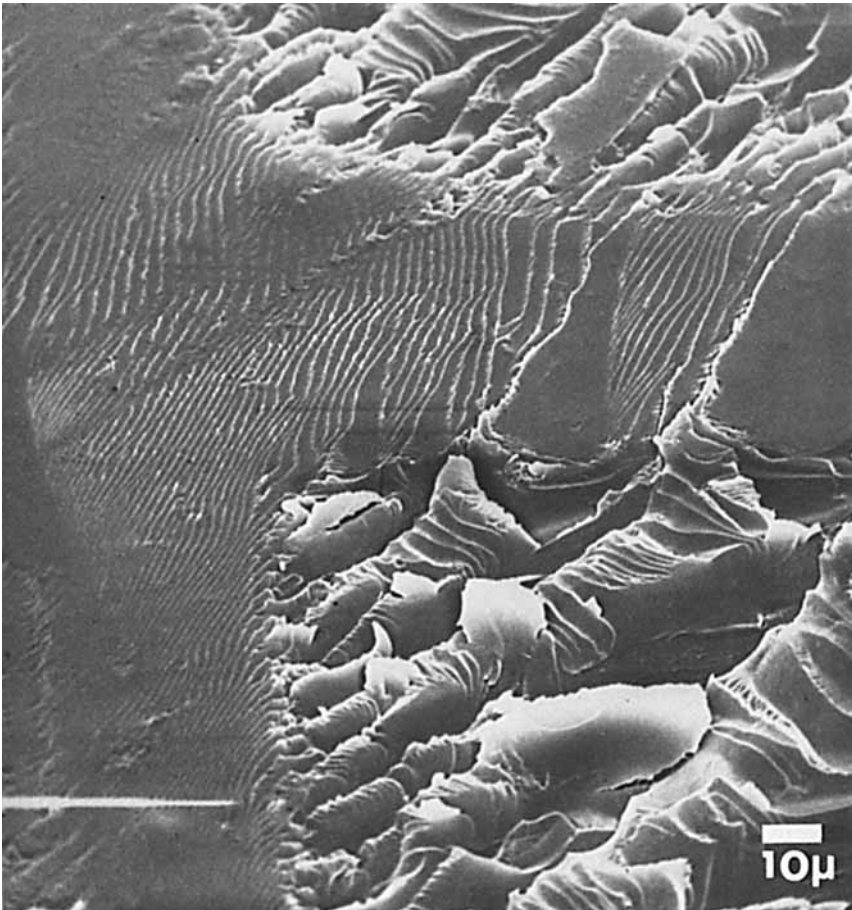


Fig. 7. SEM of surface revealed after peeling a PET film identical to that used in Fig. 6.

surface appearances (Figs. 6a and 6b). These figures confirm the observations regarding the surface texture noted in Figure 5. The effect illustrated in Figure 6 demonstrates that some volatilization appears to be taking place from the irradiated regions. A volume contraction due to crystallinity changes seems unlikely in view of the absence of surface cracks at the exposed-unexposed boundaries and the absence of density changes during irradiation.<sup>11</sup> The volatilization of low molecular weight fragments is in keeping with the IR studies indicating severe chain scission in the uppermost surface layers. The possibility of oligomers suffering secondary reactions leading to some gaseous products also exists.

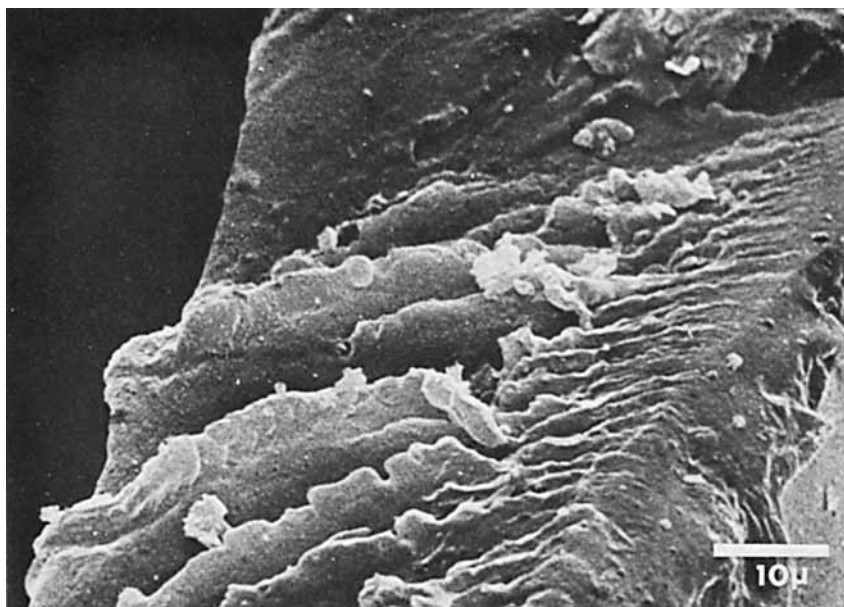


Fig. 8. Transverse fracture surface of PET film after UV irradiation for 1000 hr on the right side.

As was done with photo-oxidized polyolefins,<sup>9</sup> it is frequently possible to expose the interior of a photochemically deteriorated film by applying an adhesive on the surface and subsequently separating the film from the dry adhesive. This results in a cohesive failure between the almost intact polymer in the interior of the film and the degraded layer at the surface. This approach is feasible for PET since poly(acrylic acid) (PAA) dried at 25°C for 15 hr forms a strong bond with the polymer surface and exposes bundles of lamellae after stripping. Although an unequivocal interpretation of the exposed morphology cannot be offered here, it is sufficient in this context to point out that the texture as well as the thickness of the stripped layer varies with the degree of UV exposure. An example of this is shown in Figure 7, where a previously described "grid shadow" was PAA stripped

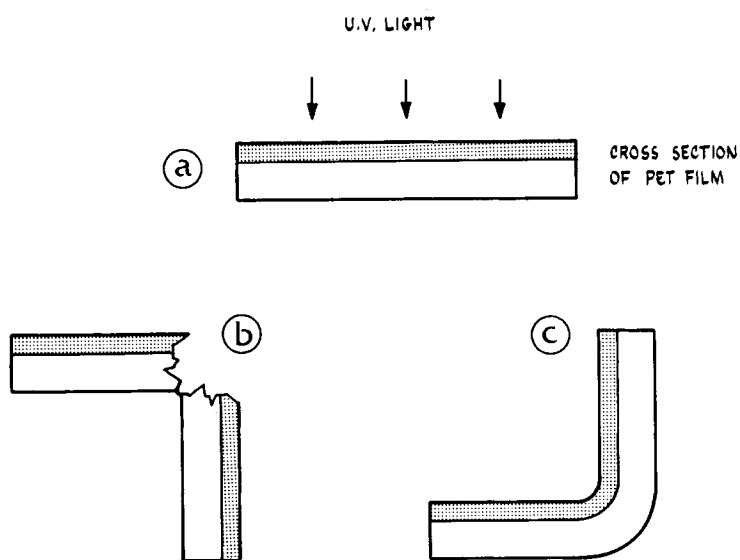


Fig. 9. Schematic diagram of flexural behavior of unilaterally UV-exposed PET film.

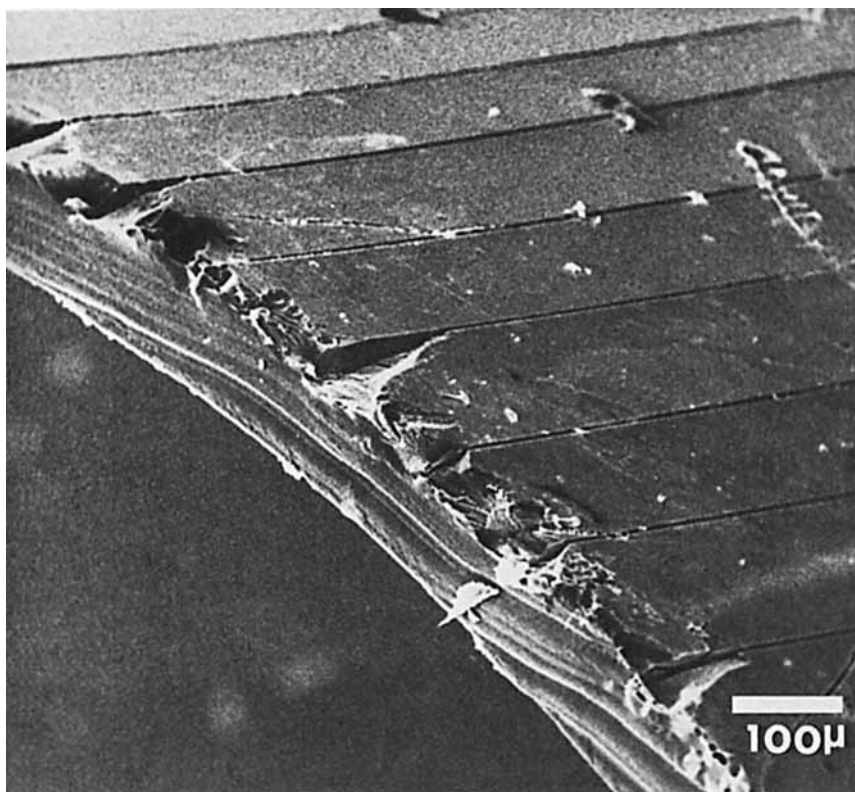


Fig. 10. SEM of convex-flexed irradiated PET film showing initiating cracks on the UV-exposed side.

to reveal different textures depending on whether the zone has been exposed to or shielded from irradiation. A different mode of cohesive failure appears to characterize the shielded PET from the exposed material.

An analogous situation is seen during tensile testing. Irradiated PET films subjected to tensile failure revealed fracture surfaces typical of that shown in Figure 8. The side exposed to the irradiation (on the right) is granular in appearance, suggestive of brittle failure, while that facing in the opposite direction appears to have the liquid-like features of a plastic deformation. This suggests that the application of tension to an irradiated film results in crack formation at the film front surface. This crack then propagates at right angles to the major stress direction through the surface degraded layer until high molecular weight polymer is encountered. The continued application of tension then results in a tearing action at the crack tip, where the stress concentrates until failure occurs.

A further illustration of this process may be seen schematically in Figure 9, where a unilaterally irradiated film is flexed convex with respect to the front face, with resulting failure (Fig. 9b) and yet survives concave flexing (Fig. 9c). This situation was examined by SEM where cracks can be seen only on the UV exposed side of the film (Fig. 10). A similar curvature imposed in reverse, leaves the sample intact.

## CONCLUSIONS

Using the ATR IR technique, it has been demonstrated that the UV-induced photochemical deterioration of PET films leads to extensive surface degradation even under moderate irradiation. On prolonged exposure, a progressive deterioration of the interior is evident. The surface nature of the UV damage is further established by showing that fluorescent degradation products are concentrated on and near the surfaces and that the mechanical properties of the deteriorated surface is grossly different from those of the interior. The photochemical reactions occurring in these surface layers are responsible for chain scission, resulting in a drastic decrease in the molecular weight of the polymeric material comprising these surface layers. It may be assumed that these chain scissions will occur in the amorphous region or at tie molecules which link the crystalline regions. Due to the relatively high glass transition temperature of the polymer ( $T_g = 67-81^\circ\text{C}$ ),<sup>12</sup> however, no appreciable reordering or restructuring may take place during irradiation to give rise to surface cracks by volume contraction. When subjected to stress, however, the applied load is now distributed mainly through the degraded areas, resulting in cracks in the surface layer. These cracks are then responsible for the initiation of fractures which propagate through the bulk of the polymer, causing tensile failure.

### References

1. M. Day and D. M. Wiles, *J. Appl. Polym. Sci.*, **16**, 203 (1972).
2. M. Day and D. M. Wiles, *J. Appl. Polym. Sci.*, **16**, 175 (1972).
3. M. Day and D. M. Wiles, *J. Appl. Polym. Sci.*, **16**, 191 (1972).
4. D. J. Carlsson and D. M. Wiles, *Can. J. Chem.*, **48**, 2397 (1970).
5. D. J. Carlsson and D. M. Wiles, *Macromolecules*, **4**, 174 (1971).
6. P. Blais, D. J. Carlsson, and D. M. Wiles, *J. Polym. Sci. A1*, **10**, 1077 (1972).
7. N. J. Harrick, *Internal Reflection Spectroscopy*, Interscience, New York, 1967.
8. N. J. Harrick and F. K. duPré, *Appl. Opt.*, **5**, 1739 (1966).
9. P. Blais, D. J. Carlsson, and D. M. Wiles, *J. Appl. Polym. Sci.*, **15**, 129 (1971).
10. J. G. Pacifici and J. M. Straley, *Polym. Lett.*, **7**, 7 (1969).
11. P. Blais, M. Day, and D. M. Wiles, to be published.
12. O. B. Edgar and R. Hill, *J. Polym. Sci.*, **8**, 1 (1952).

Received October 31, 1972

Revised November 28, 1972